

Electrochemically Fabricated Polyaniline Nanoframework Electrode Junctions that Function as Resistive Sensors

Jun Wang,^{†,‡} Samuel Chan,^{†,‡} Richard R. Carlson,^{†,‡} Yi Luo,[§] Guanglu Ge,[§]
Ryan S. Ries,[§] James R. Heath,^{*,§} and Hsian-Rong Tseng^{*,†,‡}

Crump Institute for Molecular Imaging, Department of Molecular and Medical Pharmacology, David Geffen School of Medicine at UCLA, Los Angeles, California 90095, and Caltech Chemistry, Pasadena, California 91125

Received June 9, 2004; Revised Manuscript Received July 12, 2004

ABSTRACT

In this paper, we demonstrate a template-free, site-specific, and scalable electrochemical method for the fabrication of individually addressable polyaniline nanoframework electrode junctions in a parallel-oriented array. These polyaniline nanoframeworks, which are composed of numerous intercrossing polyaniline nanowires that have uniform diameters ranging from 40 to 80 nm, can be used for the chemical sensing of HCl and NH₃ gases and ethanol vapor and for sensing the pH of aqueous NaCl solutions.

Recent developments in the design and synthesis of conducting one-dimensional (1-D) nanostructured materials, including carbon nanotubes,^{1–4} metal- and/or oxide-based nanowires,^{5–7} and polymer nanowires,^{8–10} have attracted much attention across scientific and engineering disciplines. These 1-D materials have become prime candidates for replacing conventional bulk materials in micro- and nanoelectronic devices^{11,12} and in chemical^{13–15} and biological^{15,16} sensors. Although many examples have been demonstrated of workable devices and sensors based on 1-D nanostructured materials, it remains a challenge to discover efficient, scalable, and site-specific approaches for incorporating these 1-D nanomaterials into lithographically patterned electrode junctions.

The simplest configuration of an electronic sensor is a resistive junction¹⁷ composed of two solid-state electrodes, between which is sandwiched a conducting material. The transport properties of the sensor change upon exposure of the junction to analytes, as a result of doping/dedoping interactions of the analyte molecules with the chemical building blocks of the conducting material. By applying a constant bias across this junction, the presence of analytes can be detected simply by monitoring the conducting current. In recent years, conducting polymer-based^{18–20} nanostructured materials in the shapes of thin films^{21,22} and nanowires^{9,23–25} have been utilized extensively in resistive sensors

because of their promising properties, which include high surface areas, chemical specificities, tunable conductivities, material flexibilities, and easy processing. For example, (i) polyaniline nanowires that have been obtained through a facile synthesis²⁶ or by an electrospinning method²⁵ have been incorporated into interdigitated electrodes to obtain gas-phase sensors that have excellent sensitivity, (ii) template-directed electrochemical processes²⁷ have been employed to fabricate nanowire junctions that feature robust polymer-electrode contacts, and (iii) mechanical stretching²⁸ and magnetic field-assisted assembly²⁴ processes have produced miniaturized polymer–electrode junctions. Despite the successes of these fabrication methods for preparing micro- and nanoscale sensors that incorporate conducting polymer-based nanostructured materials, there are certain limitations in terms of device yields, potential for further miniaturization, scalability, and fabrication costs that prohibit sequential developments of these types of resistive sensors. In addition, to date, most resistive sensors have been employed only for the detection of analytes in the gas phase. The ability to harness the promising properties of conducting polymer-based nanostructured materials for the development of resistive sensors that function in solution will open up new opportunities to revolutionize many conventional analytical techniques.

In this paper, we describe the use of electrochemical polymerization, at low and constant current levels, to fabricate, simultaneously and site-specifically, 10 polyaniline nanoframework-electrode junctions (PNEJs; Figure 1) in which a number of polyaniline nanowires of uniform diameter (ca. 40 to 80 nm, see Figs. 1c and d) intertwine to

* Corresponding author. E-mail: hrtseng@mednet.ucla.edu. Phone: (310) 794-1977. Fax: (310) 206-8975.

[†] Crump Institute for Molecular Imaging.

[‡] Department of Molecular and Medical Pharmacology

[§] Caltech Chemistry.

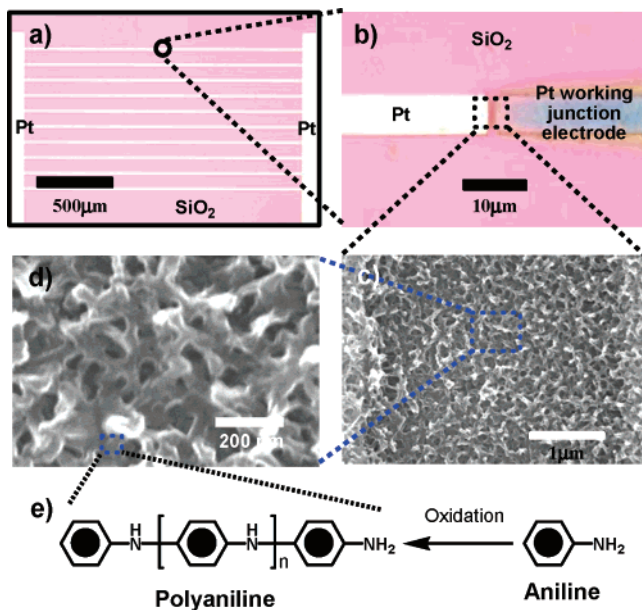


Figure 1. (a) Optical microscopy image of an electrode pattern comprising 10 pairs of junction electrodes (30-nm-thick Pt on 5-nm-thick Ti) fabricated on a silicon (100) substrate covered by a 500-nm-thick thermal oxide. (b) An optical microscopy image of a polyaniline nanoframework electrode junction (PNEJ) after site-specific electrochemical polymerization. The polyaniline nanoframework was grown precisely across the 2- μm gap between the two Pt electrodes. (c, d) Scanning electron microscopy (SEM) images of a PNEJ. The polyaniline nanoframework comprises numerous intercrossing nanowires that have diameters in the range from 40 to 80 nm. (e) Structural formula of polyaniline produced by the oxidative polymerization of aniline.

form nanoframeworks across the 2- μm gap between each pair of Pt electrodes (Figure 1b) without the necessity of using any supporting template.²⁷ Our goals were (i) to develop a highly efficient electrochemical process for the simultaneous and parallel fabrication of 10 PNEJs in an array and (ii) to use the resulting array as a set of resistive junctions to demonstrate real-time electronic sensing in the gas phase and in solution.

For the fabrication of the PNEJs, we applied a low-current electrochemical polymerization based on a well-established²⁹ template-free method for producing polyaniline nanowires. Rather than growing the nanowires ubiquitously on the surfaces of the electrodes, we chose to prepare 10 PNEJs simultaneously by growing 10 polyaniline nanoframeworks site-specifically from one set of electrodes to the other set of electrodes across 2- μm gaps. In principle, the number of PNEJs of a junction array can be scaled up without limit by increasing the number and packing density of the electrodes. Additionally, all of the resulting PNEJs can be produced simultaneously in a parallel fashion. Moreover, by addressing each individual junction electrochemically in a solution containing one specific monomer, a variety of conducting polymers can be introduced site-specifically into the polymer nanoframework–electrode junctions to create an array containing a library of different polymer nanoframework–electrode junctions. This approach should be highly efficient and scalable, while meeting the current requirements for nanoelectronics technologies, i.e., an integration of bottom-

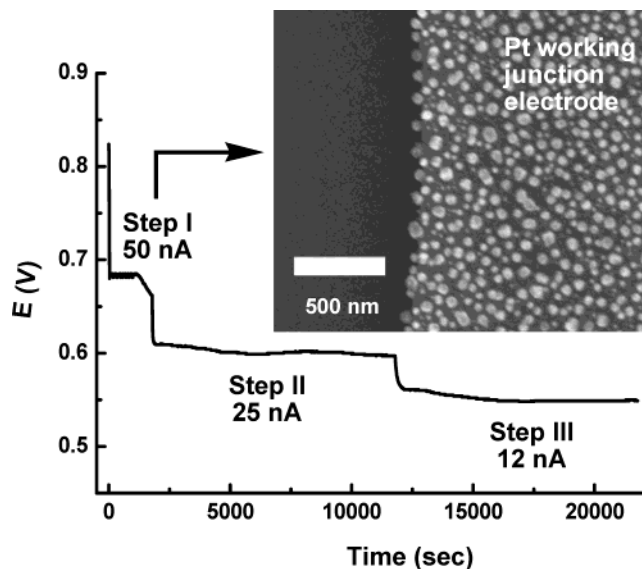


Figure 2. Plot of potential versus time for the three-step electrochemical production of PNEJs. The SEM micrograph (inset) displays the many polyaniline nuclei (20–80-nm diameter) that were generated on the working junction electrodes after the first electrochemical step at the relative high current (50 nA).

up production methods (electrochemical polymerization of nanoframeworks) and top-down fabrication (lithographic fabrication of Pt electrodes in an array).

Figure 1a displays the electrode patterns we employed for the electrochemical production of the PNEJs. We fabricated 10 pairs of electrodes (thickness: ca. 30 nm of Pt on 5 nm of Ti; width: ca. 10 μm ; length: ca. 1000 μm) by standard photolithographic techniques and using electron beam deposition on a silicon (100) substrate covered with 500 nm of thermal oxide. The spacing between the parallel electrode patterns is ca. 100 μm , and a 2- μm gap is located between the “fingertips” of each pair of electrodes. In addition, a set of 10 electrodes were connected internally to a millimeter-scale electrode pad designated for attachment of wires. Before the fabrication of the PNEJs, the electrode patterns were immersed in piranha solution (70% concentrated H₂SO₄/30% H₂O₂) for 2 min, rinsed with water, and then dried under a stream of N₂. Two sets of electrodes were then wire-bonded individually for connection to a potentiostat (Princeton 263A) and to the measurement systems. We performed the electrochemical production of the PNEJs using an aqueous solution containing 0.5 M aniline and 1.0 M HCl. We connected a standard three-port electrochemical configuration composed of working, counter, and reference electrodes to one set of junction electrodes, a Pt coil, and an Ag/AgCl reference electrode, respectively; the other set of electrodes remained unconnected. The electrochemical process we employed for the production of the polyaniline nanoframeworks within the 2- μm gaps can be divided into three continuous steps (Figure 2). In the first step, a constant current (50 nA) was applied for ca. 30 min to introduce the polyaniline nuclei onto the Pt working junction electrodes. Under this relatively high current, the effective potential on the working electrodes remains at ca. 0.68 V (vs Ag/AgCl reference electrode). It is essential to produce these initial

electrode-based polyaniline nuclei because they serve as seeds²⁹ for the growth of the nanoframeworks during the following two steps. In contrast, the use of a conventional cyclic voltammetry (CV) process results only in the formation on the electrode surface of homogeneous polyaniline thin films that lack any nanoscale features. A scanning electron microscopy (SEM) image (inset in Figure 2) of a working junction electrode obtained immediately after the first electrochemical step indicates the formation of the uniform polyaniline nuclei (diameters of ca. 20 to 80 nm). After this first step, the current was reduced to 25 nA while the effective potential dropped to 0.60 V (vs Ag/AgCl reference electrode). During the second step (180 min), the polyaniline nanoframeworks begin to propagate from the working junction electrodes to the other set of junction electrodes. Finally, the current was decreased to 12 nA, which led to an effective potential of 0.56 V. After 180 min, the 10 PNEJs were obtained simultaneously in a parallel array with each polyaniline nanoframework positioned precisely within the 2- μm gap between its electrodes. We used SEM to characterize the morphology of the polyaniline nanoframework of each PNEJ. As the SEM micrographs indicate in Figures 1c and d, the nanoframeworks are composed of numerous intercrossing polyaniline nanowires that have diameters ranging from 40 to 80 nm. The correlation between the diameters of the polyaniline nanoframeworks and those of the nuclei suggests that these nanoframeworks are most likely grown from the nuclei. Our observations are explained completely by the mechanism described previously²⁹ for the template-free production of polyaniline nanowires. In addition, we stress that our electrochemical approach to the fabrication of PNEJ arrays is highly reproducible; in fact, we have fabricated 36 PNEJ arrays successfully from 38 attempts when using processes similar to the three-step electrochemical method described above. All of these 36 PNEJ arrays are characterized by SEM and transport (I - V) studies. We found that the resulting nanoframeworks between each electrode junction have very regular dimensionalities (ca. 40 to 80 nm, see Figure 1c, d), and all of these arrays exhibit similar resistances ranging from 300 to 1000 Ω . We summarize the resistances of these PNEJ arrays as a histogram, which is shown in Figure 3.

We applied these PNEJ arrays as miniaturized resistive sensors for the real-time detection of NH_3 and HCl gases and ethanol vapor. For all measurements in these experiments, which we performed at room temperature under ambient conditions using a Keithley 4200 semiconductor analyzer, a 0.1-V bias was applied across all of the PNEJs in an array and the change in resistance [$\log(R/R_0)$, where R is time-dependent resistance and R_0 is the initial resistance] was monitored as a function of time (s). In the first of these experiments, we targeted the detection of NH_3 . A PNEJ array was first doped in 1.0 M aqueous HCl prior to measurement. Figure 4a displays the real-time change in resistance of an HCl -doped PNEJ array upon exposure to NH_3 (100 ppm) dispersed in an ambient environment. We observed an increase in resistance by 1.2 orders of magnitude within 80 s as a result of the dedoping of polyaniline by NH_3 . Because

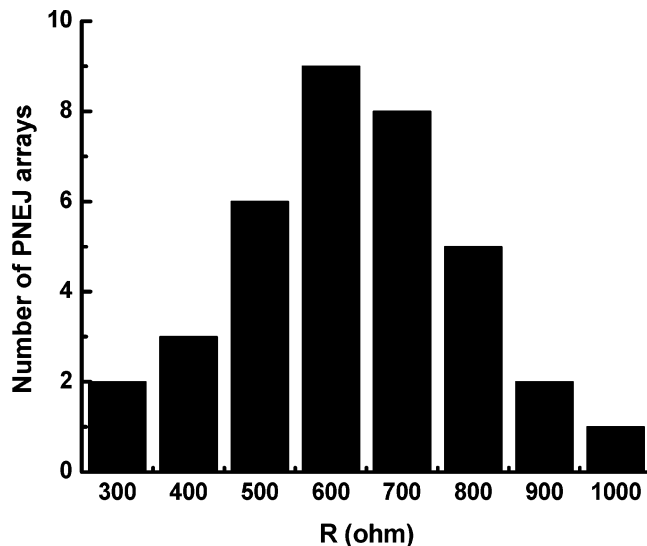


Figure 3. A histogram summarizing the resistances of 36 electrochemically fabricated PNEJ arrays.

the dedoping of polyaniline by NH_3 is a reversible process, in Figure 4b we demonstrate 10 cycles of the detection of NH_3 (0.5 ppm); this process, which occurs with high reproducibility, was performed by sequentially inserting and removing the PNEJ array in and out of a container (1.0 L) filled with 0.5 ppm NH_3 . Although the intensity of the response of the array toward NH_3 decayed with each detection cycle, we believe that this effect is due to a progressive decrease in the effective NH_3 concentration in the container because the experiment was conducted in an open system. For the detection of HCl , the same device was undoped by immersing the array in a 1.0 M NH_4OH solution. Figure 4c presents the response of the resistance of the undoped PNEJ array to HCl (100 ppm). We observed a change in resistance by 4 orders of magnitude within a response time of 5 s. The abilities of these sensors to detect acidic and basic gases are completely consistent with the results reported previously for other polyaniline-based sensors.^{23,25} In addition to NH_3 and HCl gas, we used our PNEJ arrays to detect a variety of organic vapors, including ethanol, methanol, chloroform, and acetone. Figure 4d displays an example of one of these studies in which we demonstrate the reversible and reproducible response of a PNEJ array to saturated ethanol vapor. The resistance of the nanoframework increased upon exposure to saturated ethanol vapor; we attribute this increase in resistance to the effect of swelling^{14,30} of polyaniline backbone caused by the ethanol vapor. The effects of humidity and temperature have noticeable inferences to the absolute conductances (less than 10%) of these PNEJ array sensors. Although these effects are negligible compared to the analyte-induced conductance changes, they still cause some perturbations in the realistic applications. To eliminate these humidity- and temperature-induced perturbations, the real-time responses of these PNEJ array sensors to gases and vapor were expressed in the form of relative changes (R/R_0). In this case, the effects of humidity and temperature can be normalized so that these PNEJ array sensors can be operated in ambient environment. At this

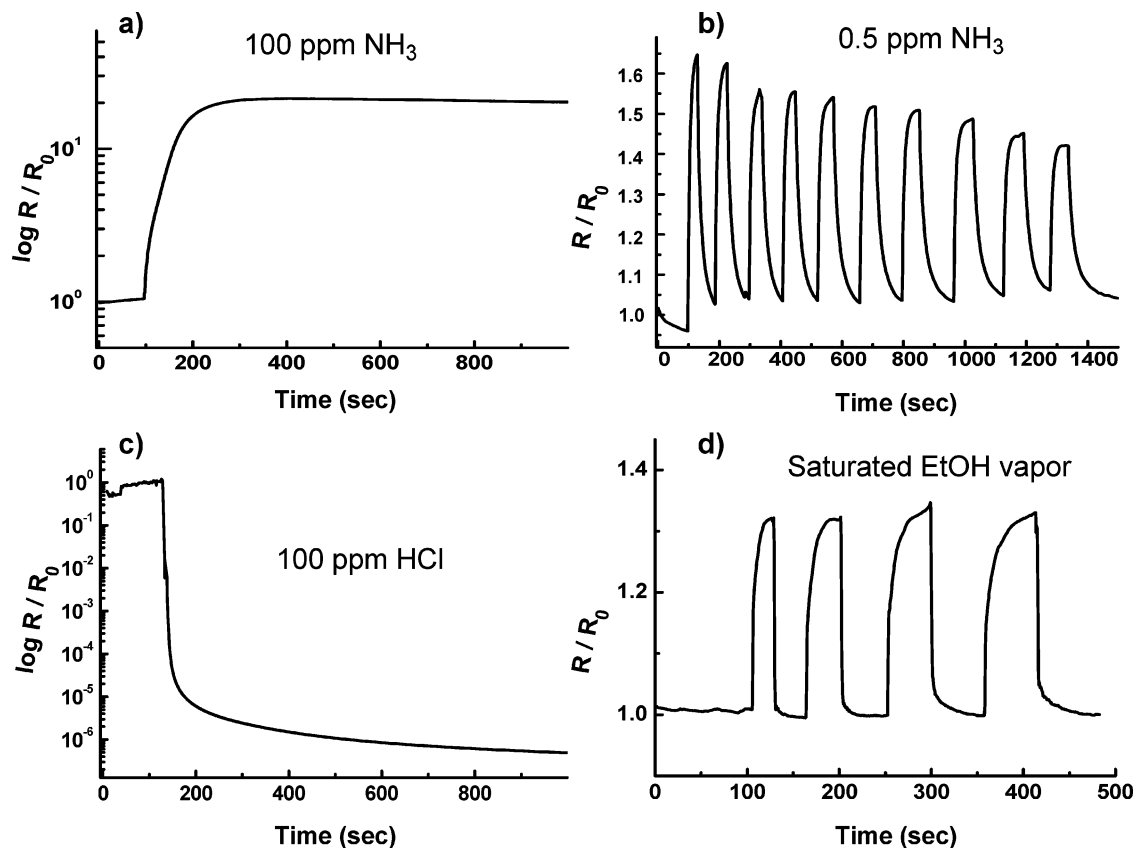


Figure 4. (a) Real-time response of a PNEJ array to the presence of NH_3 (100 ppm) under ambient conditions. (b) Reversible and reproducible response of a PNEJ array to NH_3 (0.5 ppm). The response intensities decay gradually because the experiment was performed by repeatedly placing the array in an open container (initially containing 0.5 ppm NH_3) and then removing it; this process caused the effective concentration of NH_3 within the container to decrease with time. (c) Real-time response of a PNEJ array to HCl (100 ppm). (d) Reversible and reproducible response of a PNEJ array to saturated ethanol. This experiment was performed by repeating a sequence of placing the sensor array into an open chamber equilibrated with ethanol vapor and then removing it.

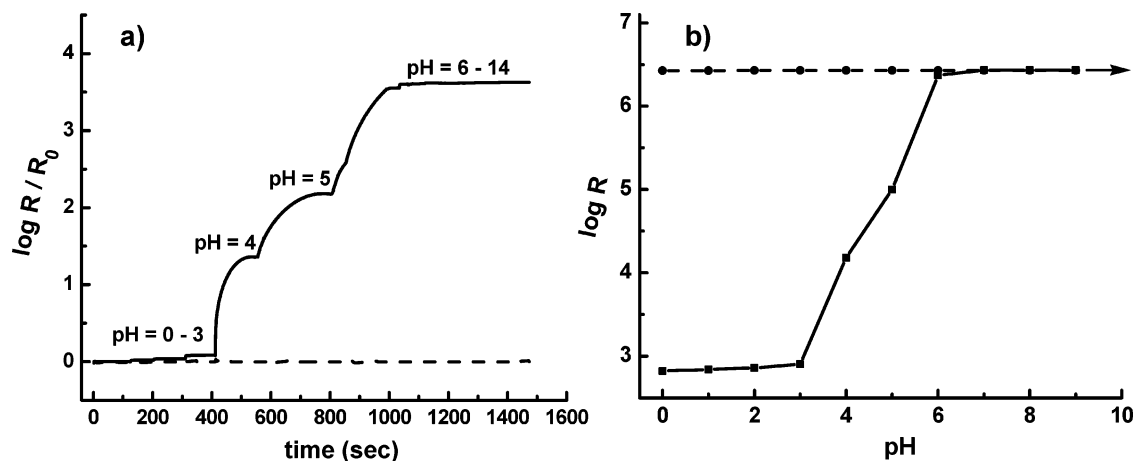


Figure 5. (a) Real-time response of a PNEJ array (solid line) and a blank device (dashed line) to NaCl solutions having different values of pH (from 0 to 14). (b) Plot of equilibrium resistance vs pH (solid line, a PNEJ array and dashed line (–) a blank device).

point, it is important to note that the experimental data shown above were collected in a research laboratory under humidity at $50 \pm 5\%$ and the temperature at $20 \pm 1^\circ\text{C}$.

In addition to sensing gases and vapors, the PNEJ arrays can also serve as sensors of the acidity of aqueous solutions. To normalize the background conductance, we prepared 15 aqueous solutions having different values of pH, ranging from 0 to 14, from a 1.0 M NaCl solution. The presences of

NaCl adjust the total ion strength of the solutions and leads to the similar background conductances for all solutions. At the same time, a blank device with no polyaniline nanoframeworks between the Pt junctions was used for measuring the conductance of the solution. The measurement was carried out by sequentially immersing the PNEJ array and the blank device into solutions having increasingly higher values of pH (i.e., from 0 to 14). Figure 5a presents the real-

time response of the resistance of the array upon its immersion into the different solutions. The response can be divided into three distinct regimes: (1) a highly doped regime (pH 0–3), where we observe less than one order increase in resistance, (2) a high-response regime (pH 3–6) where the resistance response to pH changes dramatically (ca. 3.5 order), and (3) an undoped regime (pH > 6), where the junction's conductance is too small and is overwhelmed by the background conductance of the NaCl solutions. In contrast, the background conductances measured by the blank device remain the same for all 15 solutions. In fact, the results for pH sensing (Figure 5b) obtained using our PNEJ array reflect, to a great extent, the resistance response of polyaniline to different values of pH that were reported in 1987 by MacDiarmid and co-workers.³¹

In summary, we have demonstrated a template-free, site-specific electrochemical approach to the precise fabrication of individually addressable polyaniline nanoframework electrode junctions (PNEJs) in a parallel-oriented array. In theory, the number of PNEJs in an array can be scaled up indefinitely by increasing the number and packing density of the electrodes. In addition, a library of different polymer nanoframework electrode junctions can be incorporated into an array by addressing each individual junction electrochemically in the presence of a particular monomeric precursor. Moreover, we have also demonstrated the excellent performance of the PNEJ arrays in terms of their high sensitivity and their fast response in the sensing of HCl and NH₃ gases, ethanol vapor, and the pH of NaCl solutions. Our long-term objective is to construct sensor arrays that incorporate a variety of polymer nanoframework electrode junctions for the real-time, parallel detection of a variety of analytes in both gas phase and in solution. By applying the electrochemical approach described in this paper, we envision the realization of real-time, high-throughput, highly specific sensor arrays in the not-to-distant future.

Acknowledgment. The research was supported by the Crump Institute for Molecular Imaging and by the Department of Molecular and Medical Pharmacology in the David Geffen School of Medicine at UCLA. Y.L., G.G., R.S.S., and J.R.H. acknowledge the Institute for Collaborative Biotechnologies through grant DAAD19-03-D-0004 from the U.S. Army Research Office. We thank Professor Ric Kaner and Jiaxing Huang in the Department of Chemistry and Biochemistry at UCLA for valuable discussions concerning the pH sensing experiments.

References

- (1) Dai, H. J. *Acc. Chem. Res.* **2002**, *35*, 1035–1044.
- (2) Andrews, R.; Jacques, D.; Qian D.; Rantell, T. *Acc. Chem. Res.* **2002**, *35*, 1008–1017.
- (3) Hu, J. T.; Odom, T. W.; Lieber, C. M. *Acc. Chem. Res.* **1999**, *32*, 435–445.
- (4) Venema, L. C.; Wildoer, J. W. G.; Tuinstra, H. L. J. T.; Dekker, C.; Rinzler, A. G.; Smalley, R. E. *Appl. Phys. Lett.* **1997**, *71*, 2629–2631.
- (5) Melosh, N. A.; Boukai, A.; Diana, F.; Gerardot, B.; Badolato, A.; Petroff, P. M.; Heath, J. R. *Science* **2003**, *300*, 112–115.
- (6) Xia, Y. N.; Yang, P. D. *Adv. Mater.* **2003**, *15*, 353–389.
- (7) Gudiksen, M. S.; Lauhon, L. J.; Wang, J.; Smith, D. C.; Lieber, C. M. *Nature* **2002**, *415*, 617–620.
- (8) Park, S.; Lim, J. H.; Chung, S. W.; Mirkin, C. A. *Science* **2004**, *303*, 348–351.
- (9) Huang, J. X.; Virji, S.; Weiller, B. H.; Kaner, R. B. *J. Am. Chem. Soc.* **2003**, *125*, 314–315.
- (10) Jerome, C.; Jerome, R. *Angew. Chem., Int. Ed.* **1998**, *37*, 2488–2490.
- (11) Bachtold, A.; Hadley, P.; Nakanishi, T.; Dekker, C. *Science* **2001**, *294*, 1317–1320.
- (12) Rueckes, T.; Kim, K.; Joselevich, E.; Tseng, G. Y.; Cheung, C. L.; Lieber, C. M. *Science* **2000**, *289*, 94–97.
- (13) Kong, J.; Franklin, N. R.; Zhou, C. W.; Chapline, M. G.; Peng, S.; Cho, K. J.; Dai, H. J. *Science* **2000**, *287*, 622–625.
- (14) Virji, S.; Huang, J. X.; Kaner, R. B.; Weiller, B. H. *Nano Lett.* **2004**, *4*, 491–496.
- (15) Cui, Y.; Wei, Q. Q.; Park, H. K.; Lieber, C. M. *Science* **2001**, *293*, 1289–1292.
- (16) Star, A.; Gabriel, J. C. P.; Bradley, K.; Gruner, G. *Nano Lett.* **2003**, *3*, 459–463.
- (17) Fraden, J. *Handbook of Modern Sensors*; 3rd ed.; Springer-Verlag: New York, 1996.
- (18) Shirakawa, H. *Angew. Chem., Int. Ed.* **2001**, *40*, 2575–2580.
- (19) Heeger, A. J. *Angew. Chem., Int. Ed.* **2001**, *40*, 2591–2611.
- (20) MacDiarmid, A. G. *Angew. Chem., Int. Ed.* **2001**, *40*, 2581–2590.
- (21) Janata, J.; Josowicz, M. *Nature Materials* **2003**, *2*, 19–24.
- (22) McQuade, D. T.; Pullen, A. E.; Swager, T. M. *Chem. Rev.* **2000**, *100*, 2537–2574.
- (23) Huang, J.; Virji, S.; Weiller, B. H.; Kaner, R. B. *Chem. Eur. J.* **2004**, *10*, 1314–1319.
- (24) Zhang, H. Q.; Boussaad, S.; Ly, N.; Tao, N. J. *Appl. Phys. Lett.* **2004**, *84*, 133–135.
- (25) Liu, H. Q.; Kameoka, J.; Czaplowski, D. A.; Craighead, H. G. *Nano Lett.* **2004**, *4*, 671–675.
- (26) Huang, J. X.; Kaner, R. B. *J. Am. Chem. Soc.* **2004**, *126*, 851–855.
- (27) Hatano, T.; Bae, A. H.; Takeuchi, M.; Fujita, N.; Kaneko, K.; Ihara, H.; Takafuji, M.; Shinkai, S. *Angew. Chem., Int. Ed.* **2004**, *43*, 465–469.
- (28) He, H. X.; Li, C. Z.; Tao, N. J. *Appl. Phys. Lett.* **2001**, *78*, 811–813.
- (29) Liang, L.; Liu, J.; Windisch, C. F.; Exarhos, G. J.; Lin, Y. H. *Angew. Chem., Int. Ed.* **2002**, *41*, 3665–3668.
- (30) Su, M.; Fu, L.; Wu, N. Q.; Aslam, M.; Dravid, V. P. *Appl. Phys. Lett.* **2004**, *84*, 828–830.
- (31) MacDiarmid, A. G.; Chiang, J. C.; Richter, A. F.; Epstein, A. J. *Synth. Met.* **1987**, *18*, 285–290.

NL049114P